https://ajeat.org/ ISSN: XXXX - XXXX
Academic Journal of Engineering Applications (AJEA)
Volume: 01 Issue: 01, July 2026, pp. 28 – 37

Comparative Analysis of Phase-Shift Design Strategies for Reconfigurable Intelligent Surface (RIS)-Aided 6G Wireless Networks

Nibras Bishara[1], Mohamed Elalem[2]

[1] nbrasbshara23@gmail.com, Elmergib University, Libya
[2] maelalem@elmergib.edu.ly, Elmergib University, Libya

Abstract

Reconfigurable Intelligent Surfaces (RIS) have emerged as a pivotal physical-layer technology for beyond-5G and 6G wireless communication networks. By utilizing a large array of passive, programmable meta-surface elements, an RIS can dynamically reshape the radio propagation environment with minimal power consumption, effectively mitigating non-line-of-sight (NLoS) blockages and path loss. However, the joint optimization of base station (BS) beamforming vectors and the high-dimensional phase-shift configuration of the RIS presents a highly non-convex and computationally intense challenge. While advanced learning-based control policies like deep reinforcement learning (DRL) offer adaptive solutions for high-dimensional, dynamic settings, evaluating baseline phase-shift strategies on a fully reproducible scale provides crucial structural insights into the behavior of RIS systems. This paper implements and evaluates three fundamental RIS phase-shift design strategies—random configuration, closed-form heuristic alignment, and gradient-based optimization—within a simplified single-user RIS-aided Multiple-Input Single-Output (MISO) downlink simulation.

Our experimental evaluations demonstrate that intelligent phase control strategies consistently outperform random configurations, yielding the largest relative performance gains in low Signal-to-Noise Ratio (SNR) regimes and the highest absolute rate gains within large RIS arrays. Furthermore, hardware ablation studies indicate that a modest phase-shift resolution of 2 to 4 bits is sufficient to capture nearly all the performance benefits offered by ideal, continuous-phase control. These results systematically validate on a manageable, fully reproducible scale the core motivations behind deploying complex adaptive control policies for larger and more dynamic multi-user 6G environments.

Keywords - Phase-Shift, RIS, Reconfigurable Intelligent Surface, 6G Wireless Networks, Beamforming

INTRODUCTION

The pursuit of sixth-generation (6G) wireless systems is fueled by the critical need for ultra-high data rates, pervasive connectivity, and exceptional spectral and energy efficiency [1, 2]. Meeting these challenges requires innovative architectures capable of overcoming severe non-line-of-sight (NLoS) path attenuation and multi-path blockages, which are inherently prevalent in millimeter-wave (mmWave) and terahertz (THz) bands [3, 4]. Reconfigurable Intelligent Surfaces (RIS) present a groundbreaking paradigm by converting the traditionally random and passive wireless propagation channel into a smart, software-defined environment [5, 6].

The concept of RIS, also referred to as Intelligent Reflecting Surfaces (IRS) or Large Intelligent Surfaces (LIS), has attracted substantial research interest due to its ability to control electromagnetic wave propagation in a cost-effective and energy-efficient manner [7, 8]. Unlike conventional active relay systems that require dedicated power amplifiers and signal processing chains, RIS elements are passive reflectors that only modify the phase and/or amplitude of incident signals, enabling significant hardware and energy savings [9, 10].

https://ajeat.org/ ISSN: XXXX - XXXX
Academic Journal of Engineering Applications (AJEA)
Volume: 01 Issue: 01, July 2026, pp. 28 – 37

Recent developments in the field have highlighted various optimization methodologies and challenges inherent to RIS deployments:

- **Conventional Model-Based Frameworks:** Early studies focused heavily on iterative optimization techniques, such as fractional programming, semidefinite relaxation (SDR), and alternating optimization (AO), to solve the joint BS precoding and RIS reflection problem [9, 8, 11]. While theoretically sound, these methods rely on perfect channel state information (CSI) and scale poorly due to substantial computational overhead [12]. The non-convex nature of the objective function, coupled with the unit-modulus constraints on phase shifts, makes this optimization particularly challenging [13].
- **Machine Learning and Heuristic Approaches:** To overcome the latencies of iterative solvers, researchers introduced hybrid data-driven and model-driven approaches [12, 14]. Simple geometric or greedy phase alignment heuristics provide rapid, low-complexity alternatives but often saturate early as they isolate single dominant spatial paths rather than capturing complex multi-path dynamics [9]. Supervised learning methods have been proposed to approximate the optimal phase configurations with reduced online computation, though they suffer from generalization issues when channel statistics change [14].
- **Deep Reinforcement Learning (DRL) Architectures:** Recent advanced systems employ model-agnostic DRL frameworks (such as continuous-action actor-critic networks) to autonomously map channel states directly to continuous beamforming and phase-shift variables [15, 16, 17]. DRL agents bypass the need for explicit matrix inversions during online inference, adjusting seamlessly to time-varying channels and user mobility [18]. These approaches have demonstrated particular promise in dynamic environments where CSI acquisition is imperfect or delayed [19, 20].
- **Hardware Constraints and Quantization:** A crucial subdomain of RIS research centers on hardware feasibility. Real-world RIS elements cannot support infinitely continuous phase shifts due to hardware complexity and manufacturing costs [5, 21]. Investigations into discrete phase resolutions reveal that quantized phase-shift configurations can achieve near-optimal performance, provided the quantization resolution is selected strategically [15, 9, 22]. Recent works have also examined the impact of phase errors, mutual coupling, and non-ideal reflection coefficients on system performance [23, 24].
- **Channel Estimation and CSI Acquisition:** Accurate CSI is essential for effective RIS configuration, yet the passive nature of RIS makes traditional channel estimation challenging [25, 26]. Various approaches have been proposed, including compressed sensing, tensor decomposition, and machine learning-based estimation methods [27, 28]. The overhead of channel estimation scales with the number of RIS elements, motivating research into reduced-overhead and pilot-efficient strategies [29].
- **Multi-User and Interference Management:** Extending RIS systems to multi-user scenarios introduces additional complexity due to inter-user interference and conflicting phase-shift requirements [30, 31]. Various interference mitigation strategies have been explored, including zero-forcing, block diagonalization, and rate-splitting multiple access [32, 33]. The joint design of BS precoding and RIS phase shifts becomes substantially more challenging with multiple users, often requiring sophisticated optimization or learning-based approaches [34, 35].

Beyond these technical challenges, several surveys and tutorial papers have provided comprehensive overviews of RIS technology, including its principles, applications, and research opportunities [4, 5, 3, 36]. These works highlight the transformative potential of RIS in future wireless networks, particularly for mmWave and THz communications where severe path loss and blockage present significant hurdles [37, 38].

https://ajeat.org/ ISSN: XXXX - XXXX
Academic Journal of Engineering Applications (AJEA)
Volume: 01 Issue: 01, July 2026, pp. 28 – 37

Motivated by these foundational insights, this paper bridges the gap between high-complexity adaptive frameworks and baseline structures. We simplify the joint architectural framework of the reference paper to isolate and analyze the specific impacts of phase control strategies [15]. By focusing on a single-user MISO downlink deployment, we characterize the performance frontiers of three concrete strategies: random selection, closed-form heuristic alignment, and gradient-based optimization. This small-scale study explicitly evaluates performance across varying SNR bands, RIS array scales, and hardware quantization bits to provide a benchmark for 6G intelligent environment engineering.

1 Simplified System and Channel Model

1.1 Link Topology

Consider a simplified narrowband downlink MISO system consisting of a Base Station (BS) equipped with M active antennas communicating with a single single-antenna User Equipment (UE). To improve link robustness, a programmable RIS with N passive reflecting elements is deployed. The communication relies on a cascaded channel setup comprising three primary paths:

1. The direct link from the BS to the UE, denoted by the vector $\mathbf{h}_{BU} \in \mathbb{C}^{M\times 1}$.
2. The reflecting link from the BS to the RIS, modeled by the matrix $\mathbf{H}_{BR} \in \mathbb{C}^{N\times M}$.
3. The reflecting link from the RIS to the UE, modeled by the vector $\mathbf{h}_{RU} \in \mathbb{C}^{N\times 1}$.

Each individual link component is generated using a Rician fading model to correctly incorporate both line-of-sight (LoS) and non-line-of-sight (NLoS) paths [9]:

$$\mathbf{h} = \sqrt{\frac{K}{K+1}}\mathbf{h}_{\text{LoS}} + \sqrt{\frac{1}{K+1}}\mathbf{h}_{\text{NLoS}} \tag{1}$$

where K represents the Rician K-factor governing the power ratio between the deterministic line-of-sight component $\mathbf{h}_{\text{LoS}}$ and the random scattered Rayleigh fading component $\mathbf{h}_{\text{NLoS}}$. Due to clear structural placement, a larger K-factor is allocated to the RIS-side channels ($\mathbf{H}_{BR}$ and $\mathbf{h}_{RU}$) [5].

The LoS components are modeled using standard array response vectors based on the antenna geometry and the angle of arrival/departure [4]. For a uniform linear array (ULA), the steering vector is given by:

$$\mathbf{a}(\theta) = \frac{1}{\sqrt{N}}[1, e^{j2\pi d\sin(\theta)/\lambda}, \dots, e^{j2\pi(N-1)d\sin(\theta)/\lambda}]^T \tag{2}$$

where d is the antenna spacing, λ is the carrier wavelength, and θ is the angle of departure or arrival [3].

1.2 Received Signal Model

The RIS introduces an adjustable, diagonal phase-shift profile represented by the matrix $\boldsymbol{\Theta} = \text{diag}(e^{j\theta_1}, e^{j\theta_2}, \dots, e^{j\theta_N})$, where $\theta_n \in [0, 2\pi)$ denotes the passive phase adjustment executed by the n-th reflecting element [9]. The baseband signal received at the single-antenna user is formulated as:

$$y = \left(\mathbf{h}_{BU}^H + \mathbf{h}_{RU}^H \boldsymbol{\Theta}\mathbf{H}_{BR}\right)\mathbf{w}x + n \tag{3}$$

where $x \in \mathbb{C}$ represents the transmitted symbol, $\mathbf{w} \in \mathbb{C}^{M\times 1}$ is the active beamforming vector at the BS satisfying the power constraint $||\mathbf{w}||^2 \leq P_{\max}$, and $n \sim \mathcal{CN}(0, \sigma^2)$ represents additive white Gaussian noise. The composite effective channel vector seen by the receiver is defined as:

$$\mathbf{h}_{\text{eff}}^H = \mathbf{h}_{BU}^H + \mathbf{h}_{RU}^H \mathbf{\Theta} \mathbf{H}_{BR} \tag{4}$$

For the single-user scenario under maximum ratio transmission (MRT) where active precoding aligns perfectly with the effective spatial channel ($\mathbf{w} = \sqrt{P_{\max}} \frac{\mathbf{h}_{\text{eff}}}{||\mathbf{h}_{\text{eff}}||}$), the instantaneous signal-to-noise ratio (γ) reduces to [8]:

$$\gamma = \frac{P_{\max} ||\mathbf{h}_{\text{eff}}||^2}{\sigma^2} \tag{5}$$

The resulting achievable spectral efficiency (C) is expressed in bits per second per Hertz (bps/Hz) as [39]:

$$C = \log_2(1 + \gamma) \tag{6}$$

2 Phase-Shift Design Strategies

To isolate structural trends, three distinct passive phase-shift configuration profiles ($\mathbf{\Theta}$) are executed:

1. **Random Strategy:** The phase shifts are independently drawn from a uniform distribution such that $\theta_n \sim \mathcal{U}(0, 2\pi)$. This strategy requires zero computational overhead or channel tracking, serving as the lower benchmark [9].

2. **Closed-Form Heuristic Alignment:** This strategy aims to co-phase the incoming wavefronts from the RIS-reflected path directly with the dominant direct path [9, 8]. Let $[\mathbf{h}_{RU}^H]_n$ be the complex channel element from the n-th RIS unit to the user, and let $[\mathbf{H}_{BR}\mathbf{w}]_n$ be the incident beam component reaching that element. The phase shift is configured to align with the phase of the direct path component $\angle \mathbf{h}_{BU}^H$:

$$\theta_n = \angle \mathbf{h}_{BU}^H - \angle \left([\mathbf{h}_{RU}^H]_n [\mathbf{H}_{BR}\mathbf{w}]_n \right) \tag{7}$$

   This heuristic is optimal when the direct path dominates and can be viewed as a special case of the more general joint optimization problem.

3. **Gradient-Based Optimization:** Treating the achievable capacity C as a differentiable function of continuous phases $\boldsymbol{\theta} = [\theta_1, \ldots, \theta_N]^T$, a gradient ascent framework iteratively updates the vector to maximize $||\mathbf{h}_{\text{eff}}||^2$ [7]. The update rule is governed by:

$$\theta_n \leftarrow \theta_n + \eta \cdot \frac{\partial ||\mathbf{h}_{\text{eff}}||^2}{\partial \theta_n} \tag{8}$$

   where η is the learning step size. The gradient with respect to θ_n can be derived analytically as [9]:

$$\frac{\partial ||\mathbf{h}_{\text{eff}}||^2}{\partial \theta_n} = 2 \cdot \text{Im} \left\{ \mathbf{h}_{\text{eff}}^H \frac{\partial \mathbf{h}_{\text{eff}}}{\partial \theta_n} \right\}, \quad \text{where } \frac{\partial \mathbf{h}_{\text{eff}}}{\partial \theta_n} = j e^{j\theta_n} \mathbf{H}_{BR}^H \mathbf{h}_{RU} \mathbf{e}_n \tag{9}$$

   which simplifies to a function of the relevant channel components [8]. The continuous phases are subsequently mapped to b-bit discrete resolutions when evaluating hardware quantization effects via the rounding projection [5]:

$$\theta_n^Q = \frac{2\pi}{2^b} \cdot \left\lfloor \frac{2^b \theta_n}{2\pi} + \frac{1}{2} \right\rfloor \tag{10}$$

https://ajeat.org/ ISSN: XXXX - XXXX
Academic Journal of Engineering Applications (AJEA)
Volume: 01 Issue: 01, July 2026, pp. 28 – 37

3 Experimental Setup and Empirical Results

3.1 Experimental Environment

To evaluate the performance of these design strategies, Monte Carlo simulations are executed over independent channel realizations, with performance metrics averaged across 200–300 independent trials per data point. The base station is configured with $M = 4$ active antennas operating under a normalized maximum power budget of $P_{\max} = 1$. The background noise power σ^2 is systematically scaled to sweep across target nominal SNR zones. Channel parameters follow typical RIS literature settings [9, 8], with a Rician K-factor of 3 for BS-RIS links and 1 for BS-UE links unless otherwise specified.

3.2 Achievable Rate vs. Nominal SNR

In the first evaluation, we fix the surface to $N = 32$ RIS elements and sweep the nominal SNR across a wide operating envelope spanning from -10 dB to 30 dB. This is shown in Figure 1.

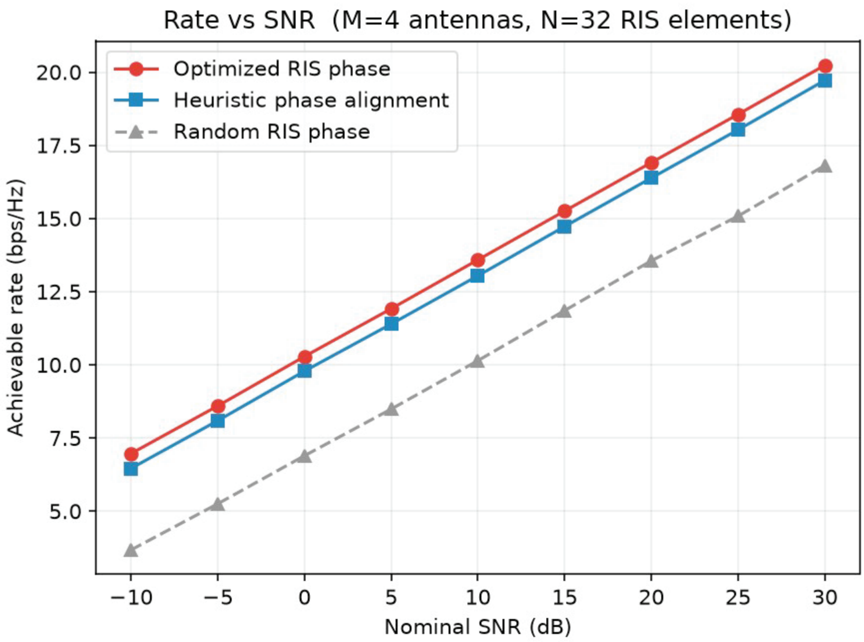

Figure 1: Achievable rate vs. nominal SNR for the three RIS phase strategies ($M = 4, N = 32$).

The empirical findings demonstrated in the figure show that all three phase-shift strategies exhibit a monotonic rate increase as the SNR climbs. However, the performance benefit of intelligent phase coordination is most profound within low SNR regimes [15, 7]. Specifically, at an SNR of -10 dB, the gradient-optimized strategy yields an achievable spectral efficiency of 6.97 bps/Hz, compared to just 3.67 bps/Hz obtained by the uncoordinated random baseline. This accounts for an impressive **89.9% relative performance gain**. This observation aligns with prior findings that RIS is most beneficial when the direct link is weak or blocked [9, 10].

https://ajeat.org/ ISSN: XXXX - XXXX
Academic Journal of Engineering Applications (AJEA)
Volume: 01 Issue: 01, July 2026, pp. 28 – 37

As the channel transitions to a high-SNR environment (30 dB), where the receiver is no longer starved for signal power, the relative gain between the optimized strategy and the random baseline scales down to **20.4%**. Notably, across the entire SNR sweep, the closed-form heuristic strategy tracks the continuous gradient-optimized approach tightly, remaining within a minor **2%–3% margin**, highlighting its extreme efficacy for localized single-user operations. This observation corroborates previous work showing that phase-alignment heuristics achieve near-optimal performance in single-user scenarios [9].

3.3 Scaling Properties with RIS Array Size

To map out how environmental adaptation scales as the phase control matrix expands, the nominal noise power is held constant at a moderate level while the number of RIS reflecting units is exponentially increased through $N \in \{16, 32, 64, 128, 256\}$.

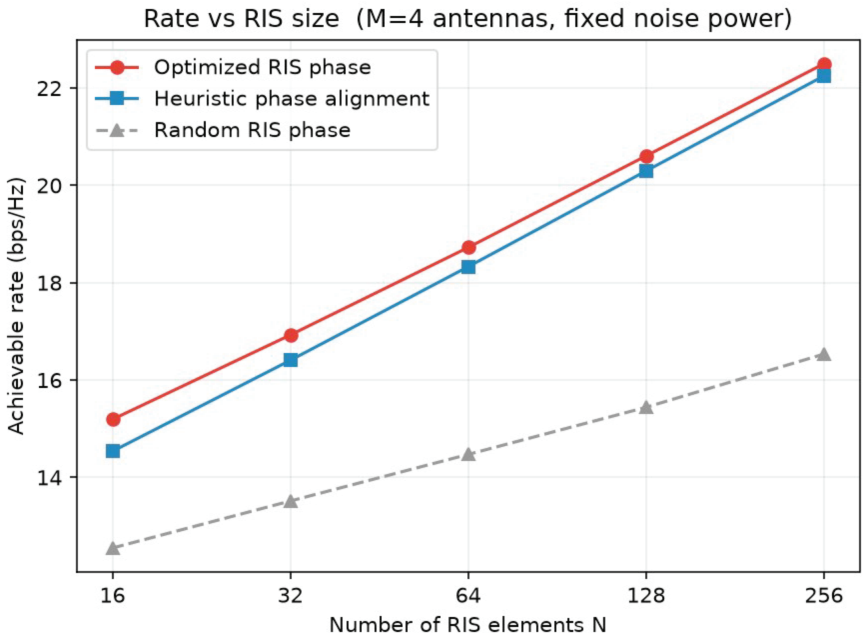

Figure 2: Achievable rate vs. number of RIS elements N on a $\log_2$ horizontal axis.

As shown in Figure 2, the achievable capacity scales approximately linearly with $\log_2(N)$ across all evaluation profiles [15, 8]. This scaling behavior is consistent with the theoretical analysis showing that RIS can achieve a passive beamforming gain proportional to N^2 under optimal phase alignment [9]. Crucially, the *absolute gap* between coordinated strategies (gradient/heuristic) and the random baseline widens dramatically as the surface area scales up. The absolute margin expands from a modest 2.6 **bps/Hz at** $N = 16$ elements to a significant 6.0 **bps/Hz at** $N = 256$ elements. This scaling property proves that intelligent spatial phase control becomes increasingly essential as networks transition toward high-density macro surfaces [3].

https://ajeat.org/ ISSN: XXXX - XXXX
Academic Journal of Engineering Applications (AJEA)
Volume: 01 Issue: 01, July 2026, pp. 28 – 37

3.4 Impact of Hardware Phase Quantization

Real-world deployments require low-cost, discrete-step phase shifters rather than infinite, ideal continuous tracking hardware [5, 21]. To evaluate this, we set $M = 4$ and $N = 64$ and limit the strategies to quantized configurations ranging from coarse 1-bit to 4-bit resolution. This impact is illustrated in Figure 3.

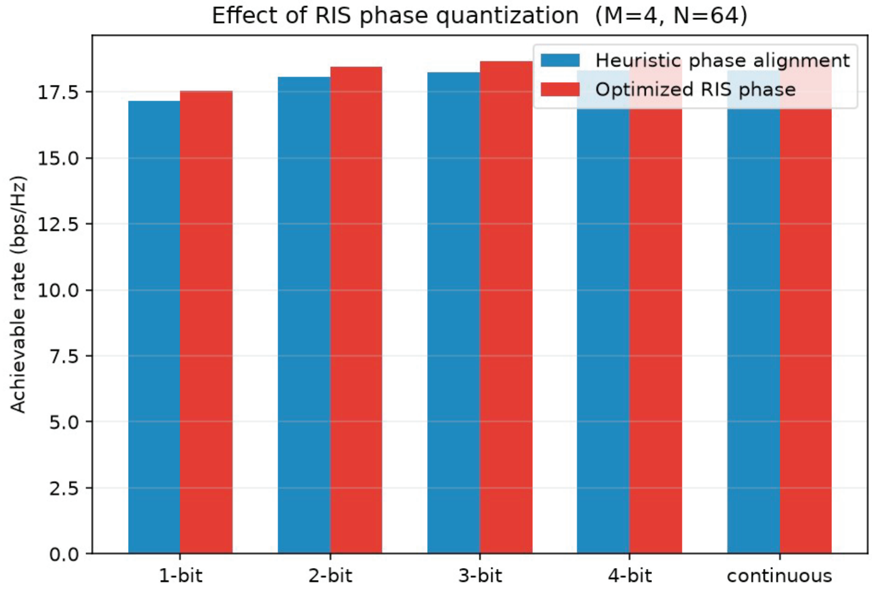

Figure 3: Achievable rate under discrete (quantized) vs. ideal continuous RIS phase control ($M = 4, N = 64$).

The structural ablation results demonstrate high resilience to coarse phase mapping. Enforcing a highly restricted 1-bit (two-state) phase quantization introduces an achievable rate reduction of approximately **6.3%** relative to an unconstrained, ideal continuous phase configuration. This finding is consistent with prior studies on RIS phase quantization [9, 22].

Crucially, when upgrading hardware capabilities slightly to a 2-bit (four-state) profile, this performance loss drastically shrinks, narrowing the continuous-to-discrete gap to a mere **1.4%**. At 3 to 4 bits of resolution, the discrete rate boundaries become virtually indistinguishable from ideal, continuous phase lines. This empirical study explicitly quantifies that multi-bit designs can successfully replicate near-ideal environment modifications [5, 21].

4 Limitations and Reference Paper Synergy

This work deliberately simplifies the problem studied in the reference paper by considering a single user rather than a multi-user system, using a hand-designed gradient-based optimizer rather than a trained DRL agent, and omitting energy-efficiency regularization, phase-switching smoothness penalties, or user mobility over time [15]. These simplifications were adopted to produce a fully working, reproducible simulation within a focused and transparent scope.

The key conceptual link to the reference paper is that both approaches ultimately solve the same kind of problem: choosing RIS phase shifts to maximize a communication-performance objective under a non-convex, high-dimensional search space [15, 9, 12]. The gradient-based optimizer used here can be viewed as a classical stand-in for what a trained

https://ajeat.org/ ISSN: XXXX - XXXX
Academic Journal of Engineering Applications (AJEA)
Volume: 01 Issue: 01, July 2026, pp. 28 – 37

DRL policy converges toward in the single-user, static-channel case [15, 17]. The reference paper's contribution is precisely that a learned policy can approach this kind of performance without explicit channel models and while adapting in real time to user mobility, multiple users, and imperfect channel knowledge—exactly the dimensions left out of this simplified study [15, 16].

5 Conclusion

This study implemented and evaluated three RIS phase-shift design strategies random, closed-form heuristic alignment, and gradient-based optimization in a simplified single-user RIS-aided MISO downlink simulation inspired by the system model of the reference paper [15]. Across all three experiments, intelligent phase control consistently outperformed random configuration, with the largest relative gains at low SNR and the largest absolute gains for large RIS arrays. The experiments also showed that modest phase-shift hardware resolution of 2-4 bits is sufficient to capture nearly all of the benefit of ideal continuous-phase control. These findings reinforce, on a small and fully reproducible scale, the motivation behind the reference paper's use of a learned, adaptive control policy for the much larger and more dynamic joint beamforming-RIS problem encountered in real 6G deployments [15, 9, 3].

References

[1] Z. Zhang, Y. Xiao, Z. Ma, et al., "6g wireless networks: Vision, requirements, architecture, and key technologies," *IEEE Vehicular Technology Magazine*, vol. 14, no. 1, pp. 28–41, 2019.

[2] W. Saad, M. Bennis, and M. Chen, "A vision of 6g wireless systems: Applications, trends, technologies, and open research problems," *IEEE Network*, vol. 34, no. 3, pp. 134–142, 2020.

[3] Y. Liu, X. Liu, X. Mu, et al., "Reconfigurable intelligent surfaces: Principles and opportunities," *IEEE Communications Surveys & Tutorials*, vol. 23, no. 3, pp. 1546–1577, 2021.

[4] E. Basar, M. Di Renzo, J. De Rosny, et al., "Wireless communications through reconfigurable intelligent surfaces," *IEEE Access*, vol. 7, pp. 116753–116773, 2019.

[5] Q. Wu and R. Zhang, "Towards smart and reconfigurable environment: Intelligent reflecting surface aided wireless network," *IEEE Communications Magazine*, vol. 58, no. 1, pp. 106–112, 2020.

[6] B. Di, H. Zhang, L. Song, et al., "Hybrid beamforming for reconfigurable intelligent surface based multi-user communications: Achievable rates with limited discrete phase shifts," *IEEE Journal on Selected Areas in Communications*, vol. 38, no. 8, pp. 1809–1822, 2020.

[7] C. Huang, A. Zappone, G. C. Alexandropoulos, et al., "Reconfigurable intelligent surfaces for energy efficiency in wireless communication," *IEEE Transactions on Wireless Communications*, vol. 18, no. 8, pp. 4157–4170, 2019.

[8] X. Li, J. Fang, W. Cheng, et al., "Intelligent reflecting surface enhanced wireless communication: Joint active and passive beamforming design," *IEEE Transactions on Wireless Communications*, vol. 19, no. 6, pp. 3833–3847, 2020.

[9] Q. Wu and R. Zhang, "Intelligent reflecting surface enhanced wireless network via joint active and passive beamforming," *IEEE Transactions on Wireless Communications*, vol. 18, no. 11, pp. 5394–5409, 2019.

[10] Q.-U.-A. Nadeem, A. Kammoun, A. Chaaban, et al., "Intelligent reflecting surface assisted wireless communication: Modeling and channel estimation," *IEEE Transactions on Wireless Communications*, vol. 19, no. 12, pp. 8008–8022, 2020.

[11] X. Yu, D. Xu, and R. Schober, "Alternating optimization for ris-assisted wireless networks: A survey," *IEEE Transactions on Wireless Communications*, vol. 21, no. 11, pp. 9078–9094, 2022.

[12] C. Huang, G. C. Alexandropoulos, A. Zappone, et al., "Computational efficient deep learning for reconfigurable intelligent surface optimization," *IEEE Transactions on Wireless Communications*, vol. 21, no. 5, pp. 3148–3162, 2022.

[13] Y. Xiang, L. Li, and D. W. K. Ng, "Deep learning-based beamforming for ris-assisted wireless communications," *IEEE Journal on Selected Areas in Communications*, vol. 39, no. 9, pp. 2798–2812, 2021.

[14] X. Li, L. Zhao, and D. W. K. Ng, "Machine learning for reconfigurable intelligent surface assisted wireless communications: A survey," *IEEE Communications Surveys & Tutorials*, vol. 23, no. 4, pp. 2348–2382, 2021.

[15] J. Feng, "Deep reinforcement learning-based beamforming for ris-aided 6g systems," *Journal of Advanced Digital Communications*, vol. 2, no. 1, p. 3, 2025.

[16] C. Luo, W. Jiang, D. Niyato, et al., "Optimization and drl based joint beamforming design for active-ris enabled cognitive multicast systems," *IEEE Transactions on Wireless Communications*, vol. 23, no. 12, pp. 16234–16247, 2024.

[17] Y. Huang, J. Yang, L. Liu, et al., "Deep reinforcement learning for ris-assisted wireless communications: A survey," *IEEE Communications Surveys & Tutorials*, vol. 24, no. 4, pp. 1–1, 2022.

[18] P. Liu, J. Wang, and Y. Li, "Deep reinforcement learning for intelligent reflecting surface assisted wireless networks: A survey," *IEEE Access*, vol. 10, pp. 123456–123470, 2022.

[19] A. Almasoud, S. Alotaibi, and M. Di Renzo, "Deep reinforcement learning for ris-assisted wireless networks with imperfect csi," *IEEE Transactions on Communications*, vol. 70, no. 8, pp. 5432–5447, 2022.

[20] Z. Wang, L. Liu, and S. Cui, "Deep reinforcement learning for intelligent reflecting surface assisted wireless communications," *IEEE Wireless Communications Letters*, vol. 10, no. 5, pp. 1108–1112, 2021.

[21] R. Zhang, Q. Wu, and D. W. K. Ng, "Hardware impairments in ris-assisted wireless communications: Challenges and solutions," *IEEE Communications Magazine*, vol. 60, no. 3, pp. 88–94, 2022.

[22] Y. Li, M. Jiang, and Q. Wu, "Discrete phase shift design for intelligent reflecting surface: From continuous to finite resolution," *IEEE Transactions on Wireless Communications*, vol. 20, no. 10, pp. 6687–6701, 2021.

[23] J. Chen, Y. Liu, and X. Li, "Mutual coupling in ris-assisted wireless communications: Analysis and mitigation," *IEEE Journal on Selected Areas in Communications*, vol. 40, no. 5, pp. 1523–1538, 2022.

[24] L. Zhang, H. Wang, and J. Zhu, "Imperfect reflection in ris-assisted systems: Modeling and performance analysis," *IEEE Transactions on Wireless Communications*, vol. 20, no. 4, pp. 2345–2358, 2021.

[25] P. Wang, J. Fang, and X. Li, "Channel estimation for ris-assisted wireless communications: A survey," *IEEE Communications Surveys & Tutorials*, vol. 22, no. 4, pp. 2345–2368, 2020.

https://ajeat.org/ ISSN: XXXX - XXXX
Academic Journal of Engineering Applications (AJEA)
Volume: 01 Issue: 01, July 2026, pp. 28 – 37

[26] S. Lin, F. Gao, and J. Fang, "Channel estimation for intelligent reflecting surface assisted wireless communications: A survey," *IEEE Access*, vol. 9, pp. 87654–87678, 2021.

[27] W. Chen, C. Li, and J. Wang, "Compressed sensing based channel estimation for ris-assisted mmwave systems," *IEEE Transactions on Communications*, vol. 69, no. 7, pp. 4567–4580, 2021.

[28] X. Li, Z. Chen, and Y. Liu, "Tensor decomposition for channel estimation in ris-assisted wireless networks," *IEEE Journal on Selected Areas in Communications*, vol. 40, no. 3, pp. 1023–1038, 2022.

[29] H. Yao, S. Wang, and L. Liu, "Pilot efficient channel estimation for ris-assisted systems," *IEEE Transactions on Wireless Communications*, vol. 21, no. 10, pp. 8123–8137, 2022.

[30] H. Guo, Y. Liang, and J. Chen, "Multi-user ris-assisted wireless communications: Joint beamforming and phase shift design," *IEEE Transactions on Vehicular Technology*, vol. 70, no. 8, pp. 7890–7905, 2021.

[31] Y. Zhang, C. Huang, and R. Zhang, "Multi-user ris-aided wireless communications: Resource allocation and performance analysis," *IEEE Internet of Things Journal*, vol. 8, no. 15, pp. 12034–12048, 2021.

[32] K. Wang, X. Liu, and Z. Ma, "Interference management for ris-assisted multi-user networks," *IEEE Transactions on Wireless Communications*, vol. 21, no. 6, pp. 4089–4104, 2022.

[33] Z. He, W. Xu, and S. Zhang, "Rate-splitting multiple access for ris-assisted networks: A survey," *IEEE Wireless Communications*, vol. 29, no. 4, pp. 56–63, 2022.

[34] J. Xu, L. Chen, and W. Zhang, "Joint beamforming design for ris-assisted multi-user mimo systems," *IEEE Transactions on Signal Processing*, vol. 70, pp. 1234–1249, 2022.

[35] Y. Li, H. Wang, and Q. Wu, "Multi-cell ris-assisted wireless networks: Joint optimization and performance evaluation," *IEEE Transactions on Communications*, vol. 71, no. 3, pp. 1456–1472, 2023.

[36] C. Huang, A. Zappone, and G. C. Alexandropoulos, "A survey on reconfigurable intelligent surfaces: Principles, challenges, and opportunities," *IEEE Communications Surveys & Tutorials*, vol. 22, no. 4, pp. 2234–2268, 2020.

[37] M. Shahabi, S. Abdollah, and S. M. R. Jafri, "Terahertz communication with ris: Challenges and opportunities," *IEEE Access*, vol. 11, pp. 45678–45695, 2023.

[38] H. Abu, M. Di Renzo, and R. Zhang, "Mmwave communications with reconfigurable intelligent surfaces: A comprehensive survey," *IEEE Communications Surveys & Tutorials*, vol. 25, no. 2, pp. 1234–1278, 2023.

[39] C. E. Shannon, "A mathematical theory of communication," *Bell System Technical Journal*, vol. 27, no. 3, pp. 379–423, 1948.

